



**HAL**  
open science

# Material slow and fast light in a zero-dispersion configuration

Bruno Macke, Bernard Ségard

► **To cite this version:**

Bruno Macke, Bernard Ségard. Material slow and fast light in a zero-dispersion configuration. 2019.  
hal-02093839v1

**HAL Id: hal-02093839**

**<https://hal.science/hal-02093839v1>**

Preprint submitted on 9 Apr 2019 (v1), last revised 17 Sep 2020 (v2)

**HAL** is a multi-disciplinary open access archive for the deposit and dissemination of scientific research documents, whether they are published or not. The documents may come from teaching and research institutions in France or abroad, or from public or private research centers.

L'archive ouverte pluridisciplinaire **HAL**, est destinée au dépôt et à la diffusion de documents scientifiques de niveau recherche, publiés ou non, émanant des établissements d'enseignement et de recherche français ou étrangers, des laboratoires publics ou privés.

# Material slow and fast light in a zero-dispersion configuration

Bruno Macke and Bernard Ségard\*

Laboratoire de Physique des Lasers, Atomes et Molécules ,  
Université de Lille et CNRS, F-59655 Villeneuve d'Ascq, France

(Dated: April 9, 2019)

We study the propagation of light pulses in an absorbing medium when the frequency of their carrier coincides with a zero of the refractive index dispersion. Although slow light and, *a fortiori*, fast light are not expected in such conditions, we show that both can be obtained by selecting particular phase-components of the transmitted field. Analytical expressions of the resulting signals are obtained by a procedure of periodic continuation of the incident pulse and a proof of principle of the predicted phenomena is performed by means of a very simple electrical network, the transfer function of which mimics that of the medium.

## I. INTRODUCTION

The one-dimensional propagation of coherent light pulses with a slowly varying envelope through a linear medium is usually analyzed by means of the group velocity [1–4]. The latter generally reads  $v_g(\omega_c) = c/[n(\omega_c) + \omega_c(dn/d\omega_c)]$  where  $\omega_c$ ,  $c$ ,  $n$  and  $dn/d\omega_c$  respectively designate the carrier frequency of the pulses [5], the light velocity in vacuum, the medium refractive index and its derivative at  $\omega_c$  (the refractive index dispersion). The dispersion can take very large values when the carrier frequency  $\omega_c$  of the pulses is equal or close to the frequency  $\omega_0$  of a narrow and well-marked resonance of the medium. When  $dn/d\omega_c > 0$  (normal dispersion), the group velocity is then very small compared to the phase velocity  $c/[n(\omega_c)]$  (slow light regime) while it becomes very large or even negative (fast light regime) when  $dn/d\omega_c < 0$  (anomalous dispersion). The principle of causality implies that the two regimes can be obtained with a same medium, depending on the detuning  $\Delta = (\omega_c - \omega_0)$  [6]. We examine in the present article what occurs when the detuning is such that  $dn/d\omega_c = 0$  (zero-dispersion configuration). Neither slow light nor fast light are expected in this case. We will however show that both can be observed by post-selecting particular phase components of the transmitted field, in analogy with the experiments involving post-selection of the field polarization [7–10]. We specifically consider the reference case of a medium with a narrow absorption line. Convincing demonstrations of slow light [11, 12] and fast light [13–17] have been performed with this system. The arrangement of our paper is as follows. In Section II, we give the transfer functions for the electric field and for its relevant phase components. The envelopes of the corresponding transmitted pulses are determined in Section III and we give in Section IV a proof of principle of the predicted phenomena by means of a very simple electrical network. We conclude in Section V by summarizing our main results.

## II. TRANSFER FUNCTIONS OF THE MEDIUM

For the sake of simplicity, we consider a dilute medium ( $n \approx 1$ ) of thickness  $\ell$  with a Lorentzian absorption line of half width at half maximum  $\gamma \ll \omega_0$ . Denoting  $\alpha$  the medium absorption coefficient on resonance *for the amplitude* ( $\alpha \ll \omega_0/c$ ), the transfer function relating the Fourier transform of the transmitted field to that of the incident field [18] then takes the simple form

$$H(\omega) = \exp \left[ -\frac{\alpha \ell}{1 + i(\omega - \omega_0)/\gamma} \right] \quad (1)$$

Notice that this result is obtained by using for the transmitted pulse a time *retarded by the luminal transit time*  $\ell/c$  (retarded time picture). This enables one to directly evidence possible fast or slow light effects. Denoting  $\Phi(\omega)$  the phase of  $H(\omega)$ , the group advance (the opposite of the group delay) is given by the relation [18]  $a_g(\omega_c) = d\Phi/d\omega|_{\omega=\omega_c}$  and reads

$$a_g(\omega_c) = \left( \frac{\alpha \ell}{\gamma} \right) \left[ \frac{1 - \Delta^2/\gamma^2}{(1 + \Delta^2/\gamma^2)^2} \right] \quad (2)$$

where  $\Delta = (\omega_c - \omega_0)$  is the detuning of the pulse carrier frequency from resonance. The group advance attains its maximum  $a_g(\omega_0) = \alpha \ell / \gamma$  for  $\Delta = 0$ , is positive (fast light regime) when  $|\Delta| < \gamma$  and negative (slow light regime) when  $|\Delta| > \gamma$ . It cancels when  $\Delta = \pm \gamma$ . We will consider in the following the case where  $\Delta = \gamma$ . Quite similar results are obtained when  $\Delta = -\gamma$ . Figure 1 shows the amplitude transmission  $|H(\omega)|$  and phase  $\Phi(\omega)$  as functions of the detuning  $\omega - \omega_0$  in the reference case  $\alpha \ell = \pi/2$ . The vertical dash-dotted line indicates the carrier frequency  $\omega_c = \omega_0 + \gamma$  considered in the following.

The use of the group velocity concept requires that the pulse envelope is slowly varying at the scale of  $1/\omega_c$ . In a frame rotating at  $\omega_c$ , the transfer function for the pulse envelopes resulting from Eq.(1) reads [5] :

$$H_\Delta(\Omega) = \exp \left[ -\frac{\alpha \ell}{1 + i(\Omega + \Delta)/\gamma} \right] \quad (3)$$

where  $\Omega \ll \omega_c$ . On exact resonance ( $\Delta = 0$ ),  $H_0(\Omega) = H_0^*(-\Omega)$ , the asterisk indicating complex conjugate. The

---

\*Electronic address: [bernard.segard@univ-lille.fr](mailto:bernard.segard@univ-lille.fr)

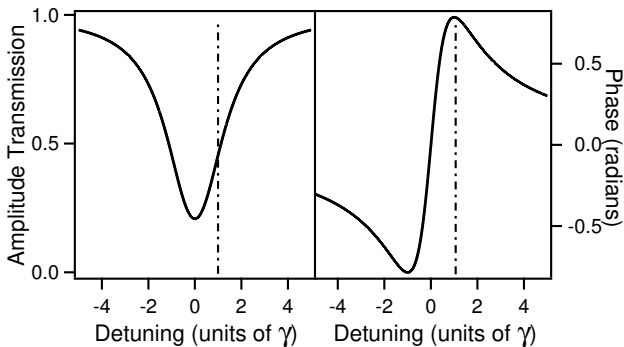


Figure 1: Modulus (on the left) and phase (on the right) of the field transfer function vs. the optical detuning ( $\omega - \omega_0$ ) for  $\alpha\ell = \pi/2$ . The vertical dash-dotted line indicates the detuning ( $\omega_c - \omega_0$ ) =  $\gamma$  of the pulse carrier considered in the article.

corresponding impulse response, inverse Fourier transform of  $H_0(\Omega)$  [18], is then real [19, 20]. If the envelope  $x(t)$  of the incident pulse is real (unchirped pulse) as assumed in the following, the envelope  $y(t)$  of the transmitted pulse will be also real or, otherwise said, the transmitted field will be in phase with the incident one [21]. An experimental evidence of this point is reported in [22]. The group advance can then be identified to the advance of the center-of-gravity of  $y(t)$  over that of  $x(t)$  while  $H_0(0)$  is the ratio of the two envelopes areas [20]. These results hold whatever the pulse distortion is.

The situation is not so simple when  $\Delta \neq 0$ . The envelope  $y(t)$  of the transmitted pulse is then complex. Its real and imaginary parts are then the envelopes of the components of the transmitted field, respectively, in phase (I) and in quadrature (Q) with the incident field. In the zero-dispersion configuration considered in the present article, the transfer functions relating the envelopes  $y_{I,Q}$  of these two components to that of the incident pulse read:

$$H_I(\Omega) = \frac{1}{2} [H_\gamma(\Omega) + H_\gamma^*(-\Omega)] \quad (4)$$

$$H_Q(\Omega) = \frac{1}{2i} [H_\gamma(\Omega) - H_\gamma^*(-\Omega)] \quad (5)$$

These transfer functions are closely related to those encountered in Ref. [10] where the post-selection was made on the field polarization. As  $H_0(\Omega)$  in the resonant case, they are such that  $H_{I,Q}(\Omega) = H_{I,Q}^*(-\Omega)$  and the envelopes  $y_{I,Q}(t)$  of the (I,Q) components are obviously real. Figure 2 shows the corresponding amplitude transmissions  $|H_{I,Q}(\omega)|$  and phases  $\Phi_{I,Q}(\omega)$  in the reference case  $\alpha\ell = \pi/2$ . Quite generally the I-transmission (the Q-transmission) is minimal (maximal) at  $\Omega = 0$  where  $H_I = e^{-\theta} \cos \theta$  and  $H_Q = e^{-\theta} \sin \theta$  with  $\theta = \alpha\ell/2$ . The group advances  $a_{gI,gQ} = d\Phi_{I,Q}/d\Omega|_{\Omega=0}$  read  $a_{gI} = (\theta \tan \theta)/\gamma > 0$  (fast light regime) and  $a_{gQ} = -(\theta \cot \theta)/\gamma < 0$  (slow light regime) [21]. The

reference case considered in Figs.(1,2) thus refers to the particular situation where  $H_I(0) = H_Q(0) = e^{-\theta}/\sqrt{2}$ ,  $a_{gI} = \theta/\gamma$  and  $a_{gQ} = -a_{gI}$ .

The previous values of  $a_{gI,gQ}$  might lead to expect that advances as large as wanted could be obtained. As in the resonant case [20], these advances are only those of the center-of-gravity of the envelopes. Anyway, obtaining large absolute advances is not an aim *per se* and the challenge in slow and fast light experiments is to attain ratios of the advances over the pulse duration as large as possible with moderate distortion. The practical limitations to these fractional advances are examined in the following section.

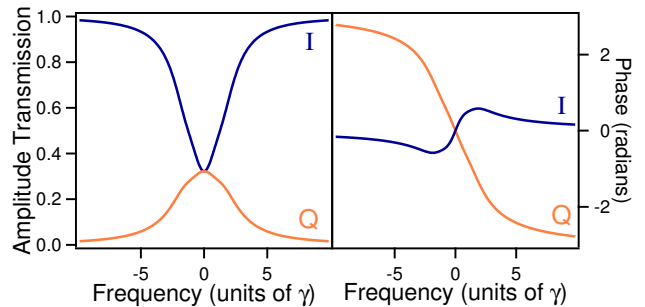


Figure 2: Same as Fig.1 for the envelope transfer functions vs. the frequency  $\Omega$ . The blue (red) line refers to the in-phase component I (the quadrature component Q). Note that, for the considered optical thickness, the group advances  $a_{gI}$  and  $a_{gQ}$  (slope of the corresponding phase at  $\Omega = 0$ ) have the same modulus but opposite sign.

### III. ENVELOPES OF THE INCIDENT AND TRANSMITTED FIELDS

We consider an incident pulse of carrier frequency  $\omega_c = \omega_0 + \gamma$  and of envelope

$$x(t) = \cos^2\left(\frac{\pi t}{2\tau}\right) \Pi\left(\frac{t}{2\tau}\right) \quad (6)$$

where  $\Pi(u)$  designates the rectangle function equal to 1 for  $-1/2 < u < 1/2$  and 0 elsewhere. This pulse is very close to the Gaussian pulse usually considered in the literature. It has a full width at half maximum  $\tau$  (taken as time unit in the following) and a strictly finite overall duration  $2\tau$ . We exploit this point by continuing the envelope  $x(t)$  at every time by the periodic signal

$$\tilde{x}(t) = \cos^2\left(\frac{\pi t}{2\tau}\right) = \frac{1 + \cos(\pi t/\tau)}{2} \quad (7)$$

$\tilde{x}(t)$  contains only three frequencies, namely 0 and  $\pm\Omega_1$  with  $\Omega_1 = \pi/\tau$ . As shows Fig.3, the signals  $\tilde{y}_{I,Q}(t)$  obtained by substituting  $\tilde{x}(t)$  to  $x(t)$  reproduce very well the main features of the exact envelopes  $y_{I,Q}(t)$  obtained

by fast Fourier transform (FFT). We get:

$$\tilde{y}_{I,Q}(t) = \frac{1}{2} \{H_{I,Q}(0) + |H_{I,Q}(\Omega_1)| \cos[\Omega_1 t + \Phi_{I,Q}(\Omega_1)]\} \quad (8)$$

$y_{I,Q}(t)$  has a maximum  $A_{I,Q} = [H_{I,Q}(0) + |H_{I,Q}(\Omega_1)|]/2$  in advance over that of the incident pulse by  $a_{I,Q} = \Phi_{I,Q}(\Omega_1)/\Omega_1$ . The corresponding fractional advances read

$$a_{I,Q}/\tau = \Phi_{I,Q}(\Omega_1)/(\Omega_1\tau) = \Phi_{I,Q}(\Omega_1)/\pi \quad (9)$$

. The advances  $a_{I,Q}$  of the maximum have the same sign that the corresponding group advances  $a_{gI,gQ}$  ( $a_I > 0$ ,  $a_Q < 0$ ). Since  $H_I(0) < |H_I(\Omega_1)|$ , the amplitude  $A_I$  of the advanced signal is larger than its asymptotic value  $H_I(0)$  when  $\Omega_1/\gamma \rightarrow 0$  ( $\gamma\tau \rightarrow \infty$ ), the opposite occurring for the amplitude  $A_Q$  of the delayed signal [ $A_Q < H_Q(0)$ ]. Equation (8) also enables us to determine the full duration at half maximum  $\tau_I$  and  $\tau_Q$  of both signals. They read

$$\tau_{I,Q} = \left(\frac{2\tau}{\pi}\right) \arccos \left[ \frac{|H_{I,Q}(\Omega_1)| - H_{I,Q}(0)}{2|H_{I,Q}(\Omega_1)|} \right] \quad (10)$$

with  $\tau_I < \tau$  (pulse narrowing) and  $\tau_Q > \tau$  (pulse broadening). All these results are consistent with those expected for systems having a dip or a peak of transmission.

In agreement with relativistic causality, both phase components start at the same time  $-\tau$  that the incident pulse (see Fig.3). As soon as it has a significant amplitude, the component  $y_Q(t)$  is simply broadened and the (negative) advance  $a_Q$  of its maximum is generally close to the group advance  $a_{gQ}$ . The behaviour of the in-phase component  $y_I(t)$  is less simple. At the first order in  $\alpha\ell$  the fractional advance  $a_I/\tau = \Phi_I(\Omega_1)/\tau$  reads

$$\frac{a_I}{\tau} = \left(\frac{\alpha\ell}{\pi}\right) \left(\frac{\Omega_1^3/\gamma^3}{4 + \Omega_1^4/\gamma^4}\right) \quad (11)$$

It attains its maximum when  $\Omega_1 = 12^{1/4}\gamma \approx 1.86\gamma$  ( $\gamma\tau = 12^{1/4}\pi \approx 1.69$ ). We then get an advance  $a_I = (3/4)^{3/4}\alpha\ell\tau/(2\pi) \approx 0.13\alpha\ell\tau$  larger than the group advance  $a_{gI} = \theta^2/\gamma$ , that is  $a_{gI} = 12^{1/4}(\alpha\ell)^2\tau/(4\pi) \approx 0.148(\alpha\ell)^2\tau$ . It should be however noticed that both advances are then extremely small. When  $\alpha\ell$  increases,  $\Omega_1 \approx 1.86\gamma$  ( $\gamma\tau \approx 1.69$ ) continues to maximize the fractional advance  $a_I/\tau$  of the maximum for moderate thickness, say  $\alpha\ell < 1.5$ . For  $\alpha\ell > 0.74$ ,  $a_I < a_{gI}$  as usual. Figure 3a shows the envelopes  $y_I(t)$  and  $y_Q(t)$  obtained in the frontier case where  $a_I = a_{gI}$ . The pulse distortion of  $y_I(t)$  is manifested in a narrowing (as above mentioned) and, moreover, in the appearance of a significant secondary lobe [20]. The latter is also well reproduced by the periodic model. Quite generally, its maximum occurs at  $t = [\pi - \Phi(\Omega_1)]/\Omega_1$  and its relative amplitude compared to that of the main lobe reads

$$D = \frac{|H_I(\Omega_1)| - H_I(0)}{|H_I(\Omega_1)| + H_I(0)} \quad (12)$$

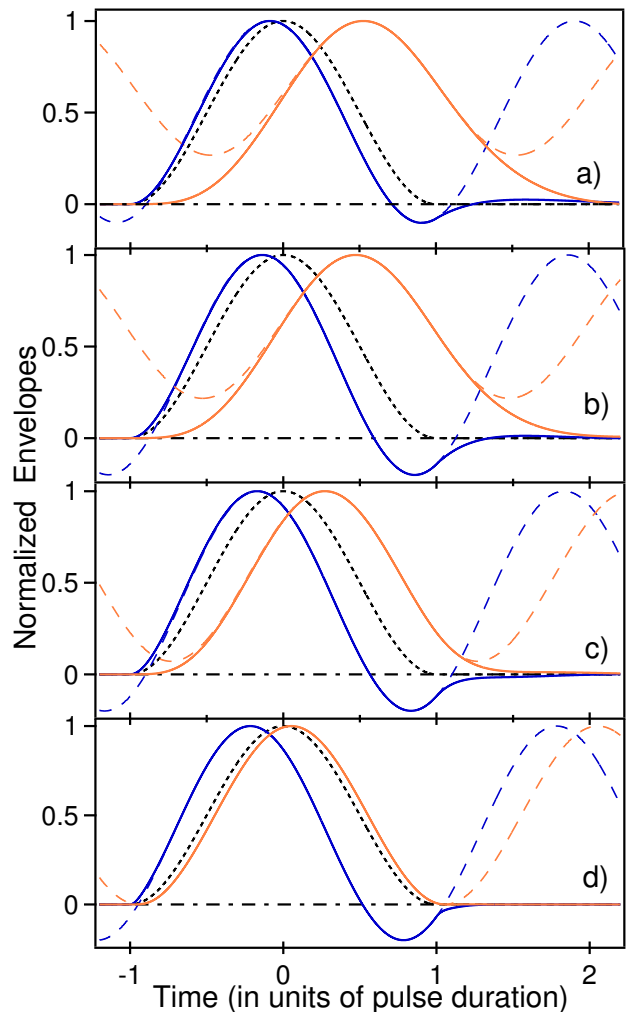


Figure 3: Normalized envelopes  $y_I(t)$  (solid blue line) and  $y_Q(t)$  (solid red line) vs. time expressed in units of the incident pulse duration  $\tau$ . The dashed lines (same colours) are the solutions obtained by periodically continuing the incident pulse. The envelope of the incident pulse (dotted black line) is given for comparison. Parameters:  $\alpha\ell$ ,  $\Omega_1/\gamma$  ( $\gamma\tau$ ) = a) 0.74, 1.86 (1.69); b) 1.18, 1.86 (1.69); c)  $\pi/2$ , 1.17 (2.68); d)  $3\pi/4$ , 0.345 (9.11).

$D$  is a good indicator of the pulse distortion. It equals 10% in the conditions of Fig.3a and raises to 20% when  $\alpha\ell \approx 1.18$  (Fig.3b). For  $\alpha\ell > 1.18$ , maximizing the advance leads to large pulse distortions,  $D$  tending to 100% when  $\alpha\ell \rightarrow \pi$ . We limit in the following  $D$  to the reasonable value 20% attained in the previous case (4% for the corresponding intensity profile). The duration  $\tau_I$  and the amplitude  $A_I$  of  $y_I(t)$  then read:

$$\tau_I = \left(\frac{2\tau}{\pi}\right) \arccos \left(\frac{D}{1+D}\right) = 0.893\tau \quad (13)$$

$$A_I = \frac{H_I(0)}{(1-D)} = 1.25 H_I(0) \quad (14)$$

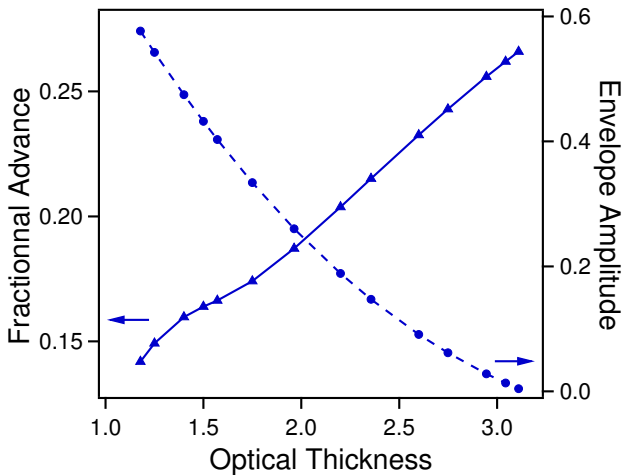


Figure 4: Fractional advance  $a_I/\tau$  (solid blue line, left scale) and amplitude  $A_I$  (dashed blue line, right scale) of the maximum of  $y_I(t)$  vs. the optical thickness  $\alpha\ell$  for  $D = 20\%$ .

For a given distortion, relativistic causality imposes severe limitations to the fractional advance  $a_I/\tau$  of  $y_I(t)$ . As for every fast light system, the larger is the dynamics of the system transmission, the larger is the fractional advance [23]. In the present case, the transmission dynamics [maximum over minimum of  $|H_I(\Omega)|$ ] is reduced to  $1/H_I(0)$ . Eq.(14) thus involves that  $a_I/\tau$  and  $A_I$  as functions of the optical thickness  $\alpha\ell$  evolve in opposite directions. Figure 4 shows the results obtained for  $D = 20\%$  when  $\alpha\ell$  varies from 1.18 (conditions of Fig.3b) to  $31\pi/32$ . In the reference case  $\alpha\ell = \pi/2$  (conditions of Fig.3c), we get  $a_I/\tau \approx 0.166$  and  $A_I \approx 0.403$  while  $a_I/\tau \approx 0.215$  and  $A_I \approx 0.147$  when  $\alpha\ell = 3\pi/4$  (conditions of Fig.3d). In the latter case, a sufficient amplitude is conciliated with a fractional advance which is not far below its asymptotic value and comparable to or even larger than those actually observed in optics [13, 15–17, 22]. For the sake of completeness, we give Fig.5 the results obtained in the conditions of Fig.4 for the delayed envelope  $y_Q(t)$ . The variations of its amplitude  $A_Q$  are moderate, while the fractional delay  $-a_Q/\tau$  continuously decreases from 0.47 for  $\alpha\ell = 1.18$  to 0 when  $\alpha\ell \rightarrow \pi$ . We additionally mention that, correlatively, the pulse duration  $\tau_Q$  (the ratio  $a_Q/a_{gQ}$ ) regularly decreases (increases) from  $1.18\tau$  to  $\tau$  (from 0.90 to 1).

When  $\alpha\ell = \pi(1 - \varepsilon)$  with  $\varepsilon \ll 1$ , it is possible to obtain explicit analytical expressions of the pulse duration  $\tau$  leading to a given value of  $D$  and of the resulting values of  $a_I/\tau$ ,  $A_I$ ,  $a_Q/\tau$  and  $A_Q$ . At the second order in  $\varepsilon$ , we get

$$\frac{\Omega_1}{\gamma} = \frac{\pi}{\gamma\tau} = \beta\varepsilon \left(1 + \frac{\varepsilon}{2}\right) \quad (15)$$

where  $\beta = 2\sqrt{D}/(1 - D)$ . That yields:

$$\frac{a_I}{\tau} \approx \frac{1}{\pi} \arctan \left\{ \beta \left[ 1 - (1 + \beta^2) \frac{\varepsilon}{2} \right] \right\} \quad (16)$$

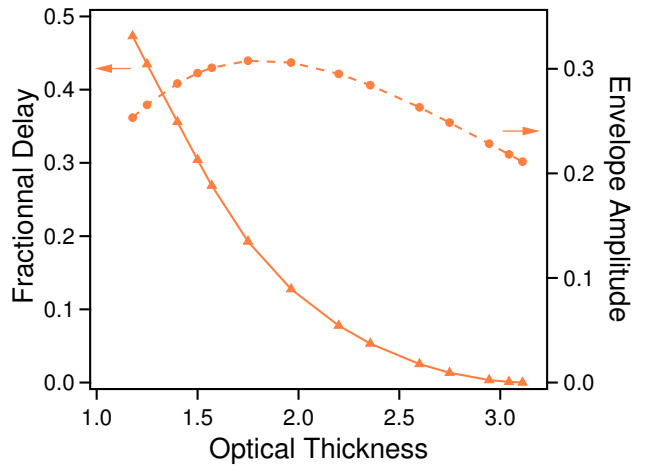


Figure 5: Same as Fig.4 for the fractional delay  $-a_Q/\tau$  (solid red line, left scale) and amplitude  $A_Q$  (dashed red line, right scale) of the maximum of  $y_Q(t)$ .

$$A_I \approx \frac{\pi e^{-\pi/2}}{4} \left(1 + \sqrt{1 + \beta^2}\right) \varepsilon \left(1 + \frac{\pi\varepsilon}{2}\right) \quad (17)$$

$$\frac{a_Q}{\tau} \approx -\frac{\beta\pi\varepsilon^2}{4} \quad (18)$$

$$A_Q \approx e^{-\pi/2} \left(1 + \frac{\pi\varepsilon}{4}\right) \quad (19)$$

For  $D = 20\%$ ,  $\beta = \sqrt{5}/2$ . We then get for  $\alpha\ell = \pi$  ( $\varepsilon = 0$ ) the following asymptotic values of the fractional advances and amplitudes, respectively,  $a_I/\tau = 0.268$ ,  $a_Q/\tau = 0$ ,  $A_I = 0$  and  $A_Q = e^{-\pi/2} \approx 0.208$ . For  $3\pi/4 < \alpha\ell < \pi$  ( $\varepsilon \leq 1/4$ ), Eqs.(16-19) yield values of advances and amplitudes equal to the exact ones within a few percent.

We finally remark that the fact that  $v_g(\omega_c) = c$  does not imply that the envelope  $|y(t)| = \sqrt{y_I^2(t) + y_Q^2(t)}$  of the total field is not advanced or delayed. This is only true in the limit where  $\Omega_1/\gamma = \pi/(\gamma\tau)$  is small enough. When  $\Omega_1/\gamma \ll 1$ , a calculation involving an expansion of  $H_I(\Omega_1)$  and  $H_Q(\Omega_1)$  at the third order in  $\Omega_1/\gamma$ , yields the following fractional advance for the maximum of  $|y(t)|$ :

$$\frac{a}{\tau} = \left(\frac{\alpha\ell}{4\pi}\right) \left(1 - \frac{\alpha\ell}{4}\right) \left(\frac{\Omega_1}{\gamma}\right)^3 = \left(1 - \frac{\alpha\ell}{4}\right) \frac{\alpha\ell\pi^2}{4\gamma^3\tau^3} \quad (20)$$

Note that this fractional advance is very small compared to that of  $y_I(t)$  which appears at the first order in  $\Omega_1/\gamma$ . In the conditions of Fig.3d, e.g.,  $a/\tau \approx 3 \times 10^{-3}$  whereas  $a_I/\tau \approx 0.215$  ( $a/a_I \approx 1.4 \times 10^{-2}$ ).

#### IV. EXPERIMENTS WITH AN ELECTRICAL NETWORK

In the fast light experiments reported in [22], the determination of an eventual phase difference between trans-

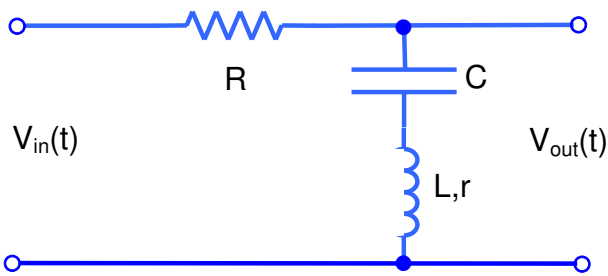


Figure 6: Electrical network used in our experiments.  $r$  designates the resistance  $r_L$  of the inductor plus an eventual additional resistance  $r_a$ . Indicative values of the parameters:  $L = 2.17 \text{ mH}$ ,  $C = 153 \text{ pF}$ , quality factor of the inductor  $Q = O(100)$  at  $\omega = 1/\sqrt{LC}$ , and  $r_a = 0$  or  $33 \Omega$ ,  $R = 1008 \Omega$  or  $365 \Omega$ .

mitted and incident fields is performed by means of frequency changes transposing the signals in the radiofrequency domain. On another hand, the phenomenon corresponding to fast light can be directly observed in the radiofrequency range by means of electrical networks with negative group delay (NGD). As back as 1961, Rupprecht [24] succeeded in evidencing significant advance of the envelope of the pulse transmitted by such a network over that of the incident pulse. See also [25]. After some lethargy, the NGD circuits have known a recent renewal of interest both in electronics and in optics. For explicit demonstrations of advanced pulse-envelope, see, e.g., [26–30].

We have used in our experiments the very simple four port network shown Fig.6. As the absorbing medium, it is purely passive. The transfer function relating the Fourier transform of the output signal  $V_{out}(t)$  to that of the input signal  $V_{in}(t)$  reads

$$H(\omega) = \frac{\eta + i(\omega - \omega_0)/\gamma}{\frac{1}{\eta} + i(\omega - \omega_0)/\gamma} \quad (21)$$

where  $\eta = \sqrt{r/(r+R)}$  ( $0 < \eta < 1$ ),  $\omega_0 = 1/\sqrt{LC}$  and  $\gamma = \sqrt{r(R+r)}/(2L)$  with  $\gamma \ll \omega_0$  (narrow resonance limit). The general relation  $a_g(\omega_c) = d\Phi/d\omega|_{\omega=\omega_c}$  giving the group advance yields

$$a_g(\omega_c) = \frac{[(1/\eta) - \eta](1 - \Delta^2/\gamma^2)}{\gamma[1 + \Delta^2/(\eta\gamma)^2][1 + (\eta\Delta)^2/\gamma^2]} \quad (22)$$

where  $\Delta = \omega_c - \omega_0$  is the detuning of the pulse carrier frequency from resonance. As for the absorbing medium, the group advance is positive when  $|\Delta| < \gamma$ , is negative when  $|\Delta| > \gamma$ , cancels when  $|\Delta| = \gamma$  and is maximum on resonance where it takes the simple form  $a_g(\omega_0) = [(1/\eta) - \eta]/\gamma$ . The experimental transmission and phase obtained for  $\eta = 0.226$ ,  $\omega_0/2\pi = 274.9 \text{ kHz}$  and  $\gamma/2\pi = 8.53 \text{ kHz}$  are shown Fig.7. They are in excellent agreement with those derived from Eq.(21). Note, however, that the values of  $\eta$ ,  $\omega_0$  and  $\gamma$  somewhat differ from those given below Eq.(21) which are obtained by

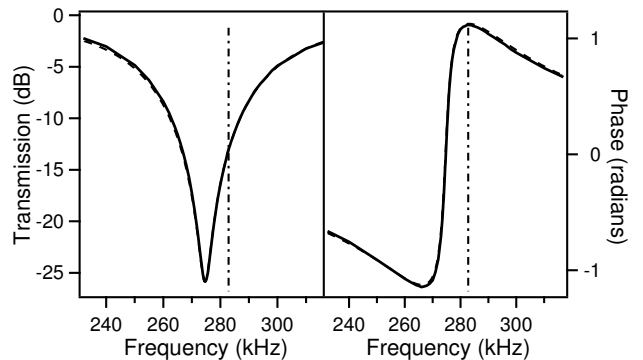


Figure 7: Transmission in dB (on the left) and phase (on the right) of the signal transfer function vs  $\omega/2\pi$  for  $r_a = 0$  and  $R = 1008 \Omega$  (solid line) and corresponding theoretical results for  $\eta = 0.226$ ,  $\omega_0/2\pi = 274.9 \text{ kHz}$  and  $\gamma/2\pi = 8.53 \text{ kHz}$  (dashed line). The vertical dash-dotted line indicates the zero-dispersion frequency  $\omega_0 + \gamma$ .

considering ideal components without including the self-resonant behaviour of the capacitor and inductor [28].

In the time-resolved experiments, we use a waveform generator (Agilent 33500B) delivering both the sinewave signal of frequency  $\omega_c$  and the modulation signal. It is used in the burst mode (single-shot experiment). The signals  $V_{in}(t)$  and  $V_{out}(t)$  are sent on two channels of a numerical oscilloscope (Keysight InfiniiVision DSOX4024A) and both are acquired on 16000 points with a 10 bit vertical resolution. Figure 8 gives an example of signals obtained in the resonant case ( $\omega_c = \omega_0$ ) with the parameters of Fig.7. As expected, the maximum of  $V_{out}(t)$  is significantly in advance over that of  $V_{in}(t)$  but the two signals are in phase [22, 25]. On the other hand, Fig.9, obtained in the zero-dispersion configuration ( $\omega_c = \omega_0 + \gamma$ ), confirms that the advance is then negligible but that the two signals are not in phase.

The transfer functions  $H_\gamma(\Omega)$ ,  $H_I(\Omega)$  and  $H_Q(\Omega)$  for the envelopes in the zero-dispersion configuration ( $\Delta = \gamma$ ) are derived from  $H(\omega)$  as those of the absorbing medium. For the electrical network  $H_\gamma(\Omega)$  reads

$$H_\gamma(\Omega) = \frac{\eta + i + i\Omega/\gamma}{1/\eta + i + i\Omega/\gamma}. \quad (23)$$

The transfer functions  $H_I(\Omega)$  and  $H_Q(\Omega)$  are deduced from  $H_\gamma(\Omega)$  by Eqs.(4,5). For the sake of completeness, we give below their values at  $\Omega = 0$  and the corresponding group advances:

$$H_I(0) = \frac{2\eta^2}{1 + \eta^2} \quad (24)$$

$$\gamma a_{gI} = \frac{(1 - \eta^2)^2}{2\eta(1 + \eta^2)} \quad (25)$$

$$H_Q(0) = \frac{\eta(1 - \eta^2)}{1 + \eta^2} \quad (26)$$

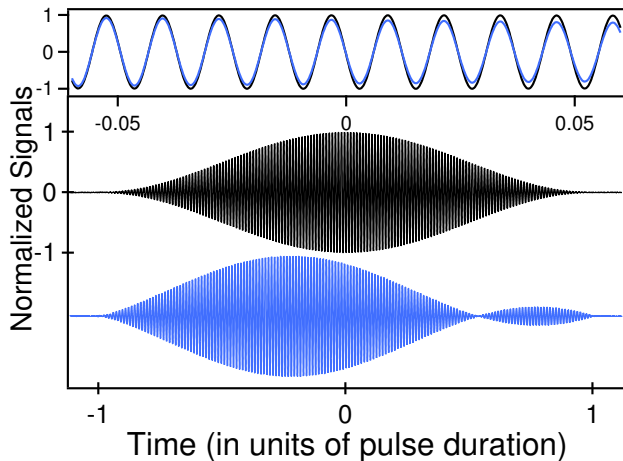


Figure 8: Normalized output signal  $V_{out}(t)$  (blue line) vs. time expressed in units of the incident pulse duration  $\tau$ . This signal is obtained in the resonant case ( $\omega_c = \omega_0$ ). The input signal  $V_{in}(t)$  (black line) is given for reference. Parameters as in Fig.7 and  $\tau = 295 \mu\text{s}$  ( $\gamma\tau = 15.8$ ). The advance of the maximum of  $V_{out}(t)$  over that of  $V_{in}(t)$  is  $a = 0.221 \tau$  (corresponding group advance  $a_g = 0.266 \tau$ ) while its relative amplitude is  $A = 0.052$ . Inset: comparison of the two signals in the vicinity of  $t = 0$  showing that they are in phase.

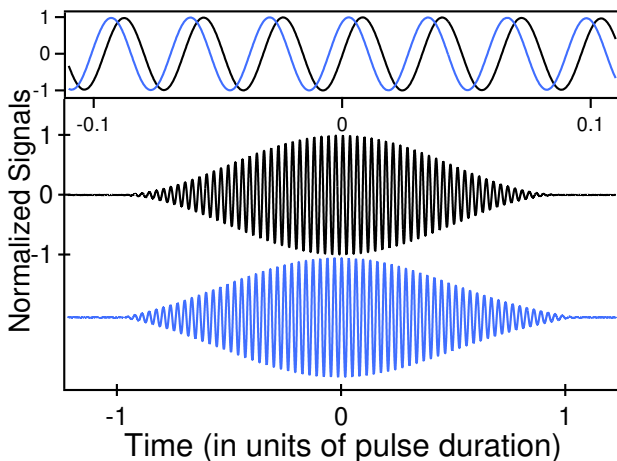


Figure 9: Same as Fig.8 in the zero-dispersion configuration ( $\omega_c = \omega_0 + \gamma$ ). The output signal has a phase differing from that of the input signal and the advance  $a$  of its maximum is negligible. The pulse duration  $\tau = 110 \mu\text{s}$  has been chosen to facilitate the comparison with the results obtained in the absorbing medium for  $D = 20\%$ . It leads to  $A = 0.224$ .

$$\gamma a_{gQ} = -\frac{2\eta}{(1 + \eta^2)} \quad (27)$$

The post-selection of the in-phase and quadrature components of the output signal  $V_{out}(t)$  is experimentally performed as follows. The data collected by the numerical oscilloscope are treated by computer. In a first step, we generate a continuous sinewave, the frequency and phase of which coincide with those of the input signal  $V_{in}(t)$ . This continuous sinewave is next multiplied by

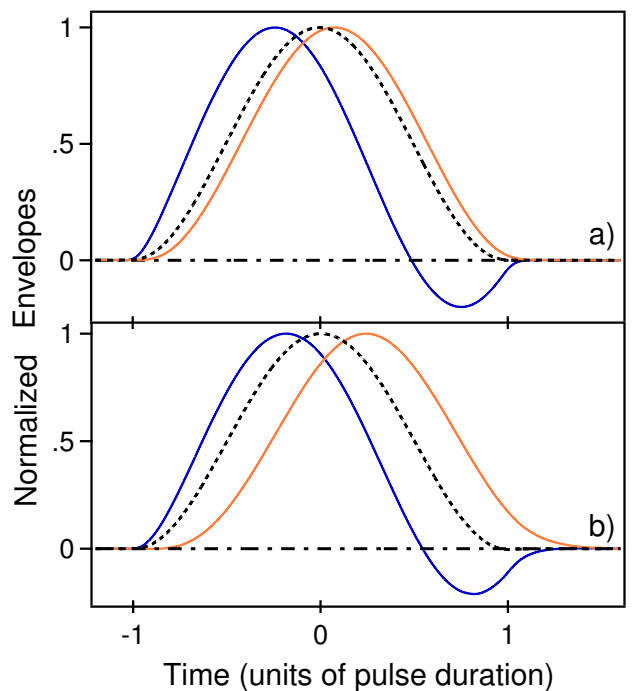


Figure 10: Two examples of envelopes  $y_I(t)$  (solid blue line) and  $y_Q(t)$  (solid red line) experimentally obtained in the zero-dispersion configuration. The envelope  $x(t)$  of the input signal (dotted black line) is given for reference. (a) is obtained in the conditions of Fig.9, viz.  $\tau = 110 \mu\text{s}$ ,  $\eta = 0.226$  and  $\gamma/(2\pi) = 8.53 \text{ kHz}$ . We get in this case  $a_I = 0.243 \tau$ ,  $A_I = 0.121$  for the in-phase component and  $a_Q = -0.074 \tau$ ,  $A_Q = 0.201$  for the quadrature component. (b) is obtained for  $\tau = 76 \mu\text{s}$  by using a circuit with resistances  $R = 365 \Omega$  and  $r_a = 33 \Omega$  leading to  $\eta = 0.450$  and  $\gamma/(2\pi) = 7.45 \text{ kHz}$ . We have in this case  $a_I = 0.200 \tau$ ,  $a_Q = -0.242 \tau$  and  $A_I/A_Q = 1.37$ .

the output signal  $V_{out}(t)$  to deliver the envelope  $y_I(t)$  of the in-phase component (I), the harmonic at  $2\omega_c$  and the high frequency noise being eliminated by a finite impulse response (F.I.R.) filter. The used low pass filter (IGOR software Blackman 367) insures a rejection better than 70 dB for  $\omega/(2\pi) > 200 \text{ kHz}$ . The envelope  $y_Q(t)$  of the quadrature component is similarly derived by using a continuous sinewave in quadrature with that used to obtain  $y_I(t)$ .

Figure 10 shows the envelopes  $y_I(t)$  and  $y_Q(t)$  experimentally observed in the zero-dispersion configuration ( $\Delta = \gamma$ ) in two representative cases. As it was made to obtain Fig.9 also as Figs.(3-5) for the absorbing medium, the durations  $\tau$  of the incident pulse are chosen such that  $D = 20\%$  for the I-component. The envelopes shown Fig.10a are observed in the conditions of Fig.9. The envelopes are quite comparable to those obtained theoretically with an absorbing medium of optical thickness  $\alpha l = 3\pi/4$  (see Fig.3d). In particular, the advance  $a_I$  is significantly larger than the delay  $-a_Q$ . On another hand, the amplitudes of the two components are such that  $A_Q/A_I \approx 1.7$  and this explains why no secondary lobe is visible Fig.9 in the over-

all envelope  $y(t) = \sqrt{y_I^2(t) + y_Q^2(t)}$ . As a second example, Fig.10b shows the envelopes experimentally observed when  $\eta = 0.450$  and  $\gamma/(2\pi) = 7.45 \text{ kHz}$ . In this case  $|a_I/a_Q|$  and  $A_Q/A_I$  are both close to unity and the envelopes are now comparable to those obtained in the case  $\alpha\ell = \pi/2$  taken as reference for the absorbing medium (see Fig.3c). In case a) as in case b), the observed envelopes are in very good agreement with the envelopes derived by FFT by using the transfer function  $H_\gamma(\Omega)$  given Eq.(23). In addition, the advances, amplitudes and pulse durations are exactly determined by the periodic model with, in particular,  $\tau_I = 0.893\tau$  and  $A_I = 1.25 H_I(0)$  as predicted by Eqs.(13,14).

## V. CONCLUSION

The dilute medium with a narrow absorption line is a reference system for the observation of fast and slow light. Fast light is obtained when the carrier frequency of the incident pulse coincides or is close to resonance while slow light is observed when this frequency lies in the line wings. There are thus two intermediate carrier frequencies for which the group velocity equals that of the light in vacuum. Paradoxically enough, we have shown that, in such a case, fast and slow light can be simultaneously observed. This is achieved by post-selecting particular phase components of the transmitted field. Fast light is obtained by selecting the component in phase with

that of a pulse travelling the same distance in vacuum while slow light is observed on the quadrature component. The general properties of fast and slow light are retrieved with this arrangement. A particular attention is paid to fast light to which the relativistic causality imposes the most severe constraints. As usual, evidencing significant fast light effects with moderate distortion requires large transmission dynamics of the medium and long incident pulses. Finally the theoretical results obtained in optics with an absorbing medium are experimentally reproduced by using a passive electrical network running in the radiofrequency range. We expect that our work will stimulate direct demonstrations in optics or microwave. In this purpose, we emphasize that the phase post-selection procedure introduced in the present article can be applied to different frequency configurations and systems.

## ACKNOWLEDGEMENTS

This work has been partially supported by the Ministère de l'Enseignement Supérieur, de la Recherche et de l'Innovation, the Conseil Régional des Hauts de France and the European Regional Development Fund (ERDF) through the Contrat de Projets État-Région (CPER) 2015–2020, as well as by the Agence Nationale de la Recherche through the LABEX CEMPI project (ANR-11-LABX-0007).

- 
- [1] W.K. Hamilton, Researches respecting Vibration, connected with the Theory of Light, Proceedings of the Royal Irish Academy 1, 341 (1839). The “velocity of propagation of vibratory motion =  $ds/dk$ ” introduced in this communication (p.348) is nothing else than the group velocity.
  - [2] L. Brillouin, *Wave propagation and group velocity* (Academic Press, New York 1960).
  - [3] C.G.B. Garrett and D.E. McCumber, Propagation of a Gaussian Light Pulse through an Anomalous Dispersion Medium, Phys. Rev. A **1**, 305 (1970).
  - [4] R.W. Boyd and D.J. Gauthier, “Slow” and “Fast light”, Prog. Opt. **43**, 497 (2002).
  - [5] All the frequencies considered in the article are angular frequencies. Lower case (upper case) letters are used to designate high (low) frequencies.
  - [6] E.L. Bolda, R.Y. Chiao, and J. Garrison, Two theorems for the group velocity in dispersive media, Phys. Rev. A **48**, 3890 (1993).
  - [7] D.R. Solli, C.F. McCormik, C. Ropers, J.J. Morehead, R.Y. Chiao, and J.M. Hickmann, Demonstration of Superluminal Effects in an Absorptionless, Nonreflective System, Phys. Rev. Lett. **91**, 143906 (2003).
  - [8] N. Brunner, V. Scarani, M. Wegmüller, M. Legré, and N. Gisin, Direct Measurement of Superluminal Group Velocity and Signal Velocity in an Optical Fiber, Phys. Rev. Lett. **93**, 203902 (2004).
  - [9] P. Bianucci, C.R. Fitz, J.W. Robertson, G. S. Shvets, and C.K. Shi, Observation of simultaneous fast and slow light, Phys. Rev. A **77**, 053816 (2008).
  - [10] B. Macke and B. Ségard, Simultaneous slow and fast light involving the Faraday effect, Phys. Rev. A **94**, 043801 (2016).
  - [11] D. Grischkowsky, Adiabatic following and slow optical pulse propagation in rubidium vapor, Phys. Rev. A **7**, 2096 (1973).
  - [12] P. Siddons, N.C. Bell, Y. Cai, C.S. Adams, and I.G. Hughes, A gigahertz-bandwidth atomic probe based on the slow-light Faraday effect, Nature Photonics **3**, 225 (2009).
  - [13] S. Chu and S. Wong, Linear pulse propagation in an absorbing medium, Phys. Rev. Lett. **48**, 738 (1982).
  - [14] B. Ségard and B. Macke, Observation of negative velocity pulse propagation, Phys. Lett. **109A**, 213 (1985).
  - [15] H. Tanaka, H. Niwa, K. Hayami, S. Furue, K. Nakayama, T. Kohmoto, M. Kunitomo, and Y. Fukuda, Propagation of optical pulses in a resonantly absorbing medium: Observation of negative velocity in Rb vapour, Phys. Rev. A **68**, 053801 (2003).
  - [16] J. Keaveney, I.G. Hughes, A. Sargsyan, and C.S. Adams, Maximal refraction and superluminal propagation in a gaseous nanolayer, Phys. Rev. Lett. **109**, 233001 (2012).
  - [17] S. Jennewein, Y.R.P. Sortais, J.F. Greffet, and A. Browaeys, Propagation of light through small clouds of

- cold interacting atoms, Phys. Rev. A **94**, 053828 (2016).
- [18] We use the definitions, sign convention and results of the linear system theory. See, for example, A. Papoulis, *The Fourier integral and its applications* (Mc Graw Hill, New York, 1987). Note that a different sign convention is often used in optics. The passage from one convention to the other is made by replacing the complex quantities by their conjugates. *The phases are then changed in their opposites* but the final results obviously do not depend on the used convention.
- [19] M.D. Crisp, Propagation of Small-Area Pulses of Coherent Light through a Resonant Medium, Phys. Rev. A **1**, 1604 (1970).
- [20] B. Macke and B. Ségard, On-resonance material fast light, Phys. Rev. A **97**, 063830 (2018).
- [21] Keep in mind that we use a retarded time picture.
- [22] Y.S. Lee, H.J. Lee, and H.S. Moon, Phase measurement of fast light pulse in electromagnetically induced absorption, Opt. Express **21**, 22464 (2013).
- [23] B. Macke, B. Ségard, and F. Wielonsky, Optimal superluminal systems, Phys. Rev. E **72**, 035601(R) (2005).
- [24] W. Rupprecht, *Lineare Netzwerke mit negativer Gruppenlaufzeit*, Dissertation. (Technische Hochschule Karlsruhe, 1961). See Fig. 5.18b.
- [25] K. Steinbuch and W. Rupprecht, *Nachrichtentechnik: eine einführende Darstellung* (Springer, Berlin 1967). See Fig.6.22.
- [26] M. W. Mitchell and R. Y. Chiao, Causality and Negative Group Delays in a Simple Bandpass Amplifier, Am. J. Phys **66**, 14 (1998).
- [27] H. Cao, A. Dogariu, and L.J. Wang, Negative Group Delay and Pulse Compression in Superluminal Pulse Propagation, IEEE J. Sel. Top. Quantum Electron. **9**, 52 (2003).
- [28] O. F. Siddiqui, S. J. Erickson, G. V. Eleftheriades, and M. Mojahedi, Time-Domain Measurement of Negative Group Delay in Negative-Refractive-Index Transmission-Line Metamaterials, IEEE Trans. Microw. Theory Techn. **52**, 1449 (2004).
- [29] B. Ravelo, “Methodology of elementary negative group delay active topologies identification”, IET Circuits Devices Syst. (CDS) **7**, 105 (2013).
- [30] B. Ravelo, Similitude between the NGD function and filter gain behaviours, Int. J. Circ. Theor. Appl. **42**, 1016 (2014).